



## Journal of Advanced Research in Fluid Mechanics and Thermal Sciences

Journal homepage:  
[https://semarakilmu.com.my/journals/index.php/fluid\\_mechanics\\_thermal\\_sciences/index](https://semarakilmu.com.my/journals/index.php/fluid_mechanics_thermal_sciences/index)  
ISSN: 2289-7879



# Study of the Characteristics of Ship Propulsion Systems with the Addition of a Kort Nozzle using the CFD Method

Alamsyah<sup>1,\*</sup>, Anggoronadhi Dianiswara<sup>2</sup>, Muhammad Uswah Pawara<sup>1</sup>, Olga Dandi Hutagaol<sup>1</sup>, Faisal Mahmuddin<sup>3</sup>

<sup>1</sup> Department of Naval Architecture, Institut Teknologi Kalimantan, 76127 Balikpapan, East Kalimantan, Indonesia

<sup>2</sup> Department of Ocean Engineering, Institut Teknologi Kalimantan, 76127 Balikpapan, East Kalimantan, Indonesia

<sup>3</sup> Department of Marine Engineering, Faculty of Engineering, Hasanuddin University, Makassar, Indonesia

### ARTICLE INFO

#### Article history:

Received 10 May 2024

Received in revised form 20 August 2024

Accepted 29 August 2024

Available online 15 September 2024

#### Keywords:

Propeller; Kort nozzle; CFD; drag force; lift force; thrust; efficiency

### ABSTRACT

The component of a ship that affects its speed the most is its propulsion system, which includes a propeller. The propeller produces thrust by converting the blades' rotating force. A well-functioning propulsion system increases the propeller's effectiveness, which enhances the ship's performance. The addition of a kort nozzle to the propeller is one of the numerous methods currently available for enhancing its performance. These justifications serve as the foundation for this investigation. The purpose of this study was to compare the propeller's operating efficiency with and without a koert nozzle addition. The result of the research it was detected that there was an increase in thrust force after using the cort nozzle under the influence of calm water and wavy water by 15 ~ 30%. There is an increase in efficiency under the influence of still water. But under the influence of waves the value is not great. The resulting efficiency value is approximately 3 ~ 5% for the same RPM rotation efficiency.

## 1. Introduction

A kort nozzle propeller is a propeller that has a channel (duct) in the form of foil that surrounds the propeller to form a casing or tube (nozzle) [1]. The phenomenon that occurs in a propeller enclosed in a tube (kort nozzle) is that the speed of the water flow inside the tube is faster than the water flow outside the tube, which results in the pressure inside the tube being lower than the pressure outside the tube. The difference in pressure results in an increase in thrust; with the installation of a kort nozzle, there is an increase in thrust. The propulsion system, or drive system, is the system that has the most influence on the ship's maneuvering process. The ship's main propulsion system is: 1. the main engine as the first mover; 2. the propeller, which generally uses a screw propeller; and 3. the transmission components, which include the shaft and reduction gear [2,3]. To make the basic shape of the propeller, a hydrodynamic shape is needed, which is also called a

\* Corresponding author.

E-mail address: [alamsyah@lecturer.itk.ac.id](mailto:alamsyah@lecturer.itk.ac.id)

<https://doi.org/10.37934/arfmts.121.1.226238>

hydrofoil. The hydrofoil will produce a lifting force that is greater than the drag, where the hydrofoil moves with a fluid medium at a speed that allows hydrodynamics to occur [4,5]. Hydrodynamics is a difference that occurs at the top and bottom of the hydrofoil. The fluid at the top of the airfoil moves faster than the fluid at the bottom of the airfoil. This is due to the pressure difference between the fluid flow at the top and the fluid flow at the bottom. As is known, the amount of pressure is inversely proportional to the amount of speed, so that the fluid flow through the bottom of the hydrofoil is smaller than the top [6].

The most frequently or commonly used propeller is the screw propeller. Screw propellers usually have two or more blades protruding from the hub or boss, where the boss is connected to a shaft driven by the main mover or main engine. Some propeller blades are integrated with the hub, and some can be installed and removed from the hub [7]. The propeller is placed as low as possible on a stand at the back of the ship. The propeller must have a center line or diameter that is made in such a way as to avoid the occurrence of the phenomenon of air drawing and propeller racing when the ship experiences pitching. A duct is a shell-shaped structure that is usually used to increase thrust and force lift in ship propulsion systems. Ducts are usually located in front of the ship's propeller and have a circular or similar shape. There are advantages and disadvantages to using a Kort nozzle, including high thrust force and very good efficiency for tugboats and pusherboats. The decrease in propeller efficiency on sea routes is smaller for the propeller. A comparison of the performance of a Kort nozzle with an open propeller is shown in Figure 1. There are two types of Kort Nozzle, which can be seen in Figure 2.

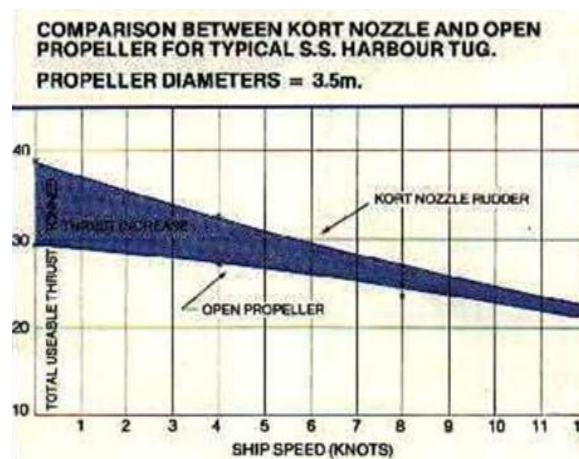


Fig. 1. Comparison graph of Kort nozzle performance compared to open propeller [8]



Fig. 2. Tipe kort nozzle, (left) Rotation nozzle view and (right) Fixed nozzle view [9]

The Kort Nozzle is a foil-shaped plate that functions as a propeller protector. The function of the nozzle is to concentrate and increase the flow of water flowing through the propeller so that it can maximize the amount of water sucked in by the propeller. Apart from maximizing the performance of the propeller, the kort nozzle can also reduce the noise and vibrations produced by the propeller's rotation. A Kort nozzle propeller is a propeller that has a channel (duct) in the form of foil that surrounds the propeller to form a casing or tube (nozzle) [1]. The phenomenon that occurs in a propeller enclosed in a tube (kort nozzle) is that the speed of the water flow inside the tube is faster than the water flow outside the tube, which results in the pressure inside the tube being lower than the pressure outside the tube. The difference in pressure results in an increase in thrust. With the installation of a kort nozzle, there is an increase in thrust.

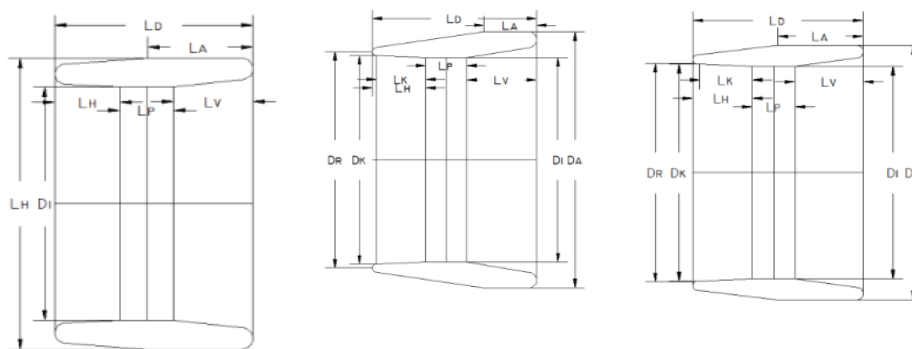


Fig. 3. Kort Nozzle Shunkshin Type A (left), B (center), and C (right) [10]

## 2. Methodology

In this study, the object of research is the B4-100 type B-series propeller design. This type of propeller has been widely studied regarding its performance as well as other types using CFD [2,11-16]. The type of data used in this research is secondary data. The data in this research includes data on the size of the B4-100 propeller design specifications. The type of propeller carried out in the analysis is the B4-100 type B-series propeller design, which has been designed using the KT-KQ-J diagram with the following specifications in Table 1:

Particular	Value
Diameters	4.37 m
pitch	1.66 m
P/D	0.86 m
Ae/Ao	1
Number of blades	4

The general research flow is shown in Figure 4 as follows

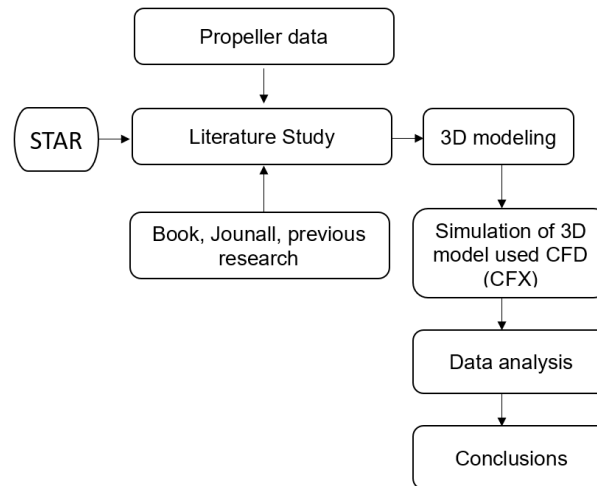


**Fig. 4.** Research of flow

In the research, an analysis of the forces acting on the propeller and the fittings of the nozzle cort is carried out, which are shown as follows

$$F = F_{\text{lift}} \cos \theta - F_{\text{drug}} \cos \theta \quad (1)$$

where  $\theta$  is angle of pitch in degree,  $F$  is thrust in kN,  $F_{\text{lift}}$  is the lift force in kN,  $F_{\text{drug}}$  is the drug force in kN. In calculating torque is use Eq. (2).

$$\tau = r \times F \quad (2)$$

where  $\tau$  is torque in kN.m,  $r$  is moment of arm in m,  $F$  is the force in kN. In calculating drug force is use Eq. (3).

$$F = \tau \times A \quad (3)$$

where  $F$  is drug force in kN,  $\tau$  is wallshear in Pa,  $A$  is the area in  $\text{m}^2$ . In calculating lift force is use Eq. (4).

$$F = P \times A \quad (4)$$

where  $F$  is lift force in kN,  $P$  is pressure in Pa,  $A$  is the area in  $\text{m}^2$ .

The method used in this research is CFD. Several studies use the same method with different outputs, such as analyzing ship resistance based on the shape of its bow, the movement of a ship under the influence of wave periods, and test the performance of the shape and type of SPOB ship rudder leaf [6,17,18]. Likewise, seakeeping and ship maneuvers can be analyzed using CFD [5]. This method is considered to be a fairly comprehensive method for studying the characteristics of a construction or object when it interacts with fluids.

### 3. Results

The propeller was drawn using Solidwork 2016 software with 3D coordinate points from calculations carried out on Hydrocomp PropCad. This process aims to make the propeller model solid.

The propeller model using Shushkin nozzles A, B, and C can be seen in Figure 5, Figure 6, Figure 7, and Figure 8 below:

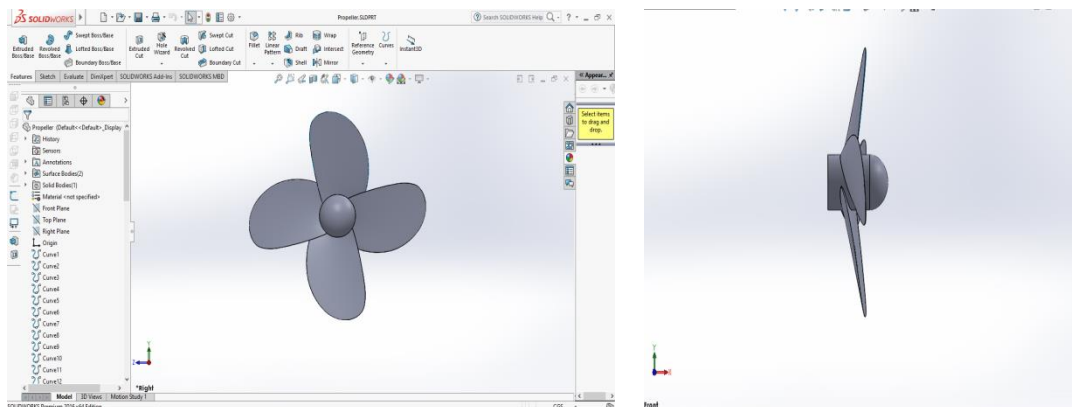


Fig. 5. Conventional of propeller

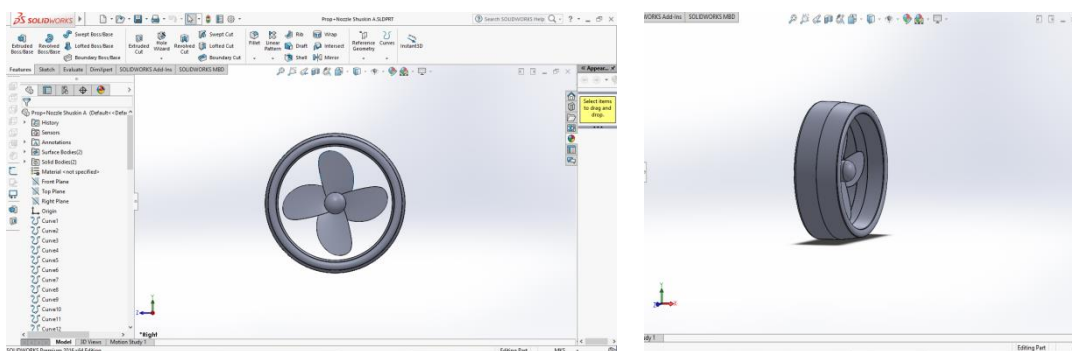


Fig. 6. Kort nozzle type A

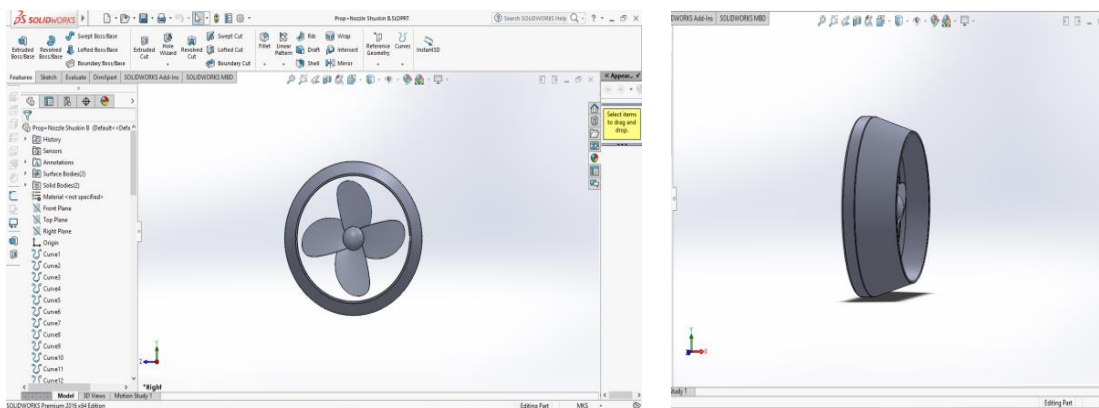


Fig. 7. Kort nozzle type B

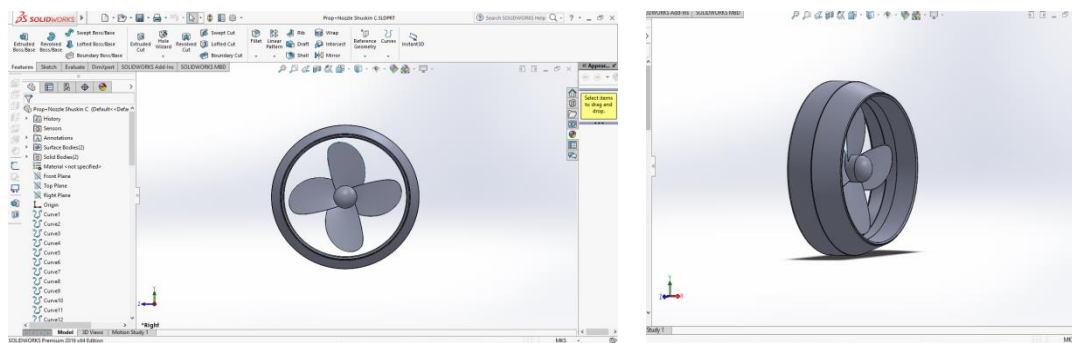


Fig. 8. Kort nozzle type C

After the modeling is complete, the next step is to carry out a CFD (computational fluid dynamics) simulation process using software to simulate fluid flow based on numerical simulation. The following are the steps in carrying out the CFD simulation process on Ansys CFX [19]. The geometry stage is the process of inputting the design and also checking whether the model that has been designed is solid or not. The geometry stage is also the stage for creating a fluid domain where a design can be tested [20]. The results of the geometry depiction can be seen in Figure 9 as follows

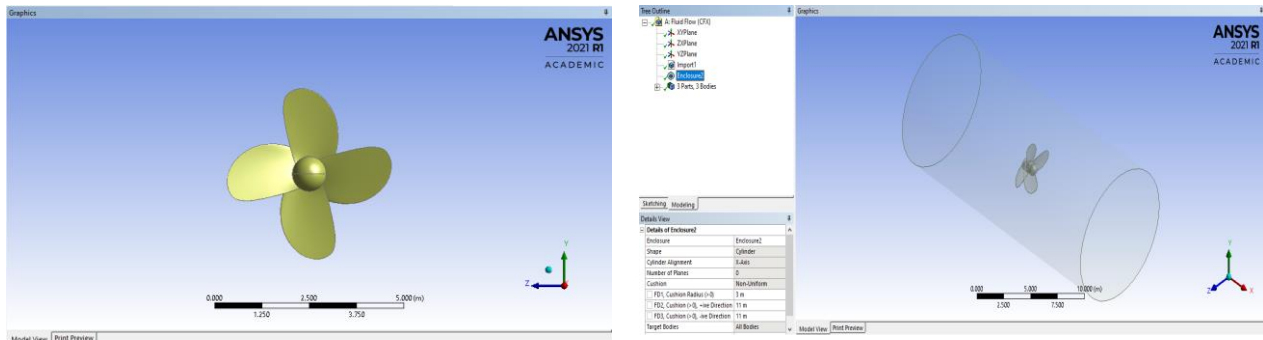


Fig. 9. Geometry and boundary layer

Next, the mesh setup is done in the "details of mesh" tool box. In this study, the mesh size used for meshing was 1.2 mm. Please note that the smaller the mesh size used, the more accurate the results of the research carried out will be [21-23]. However, it takes longer when meshing and must also be supported by capable devices. The results of meshing can be seen in Figure 10 as follows

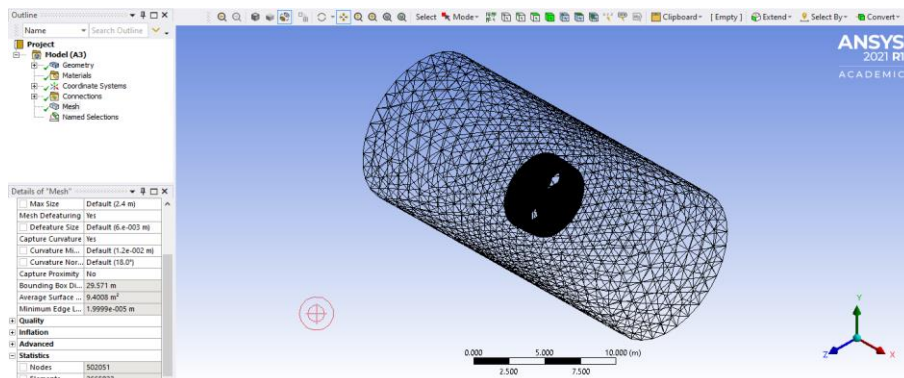
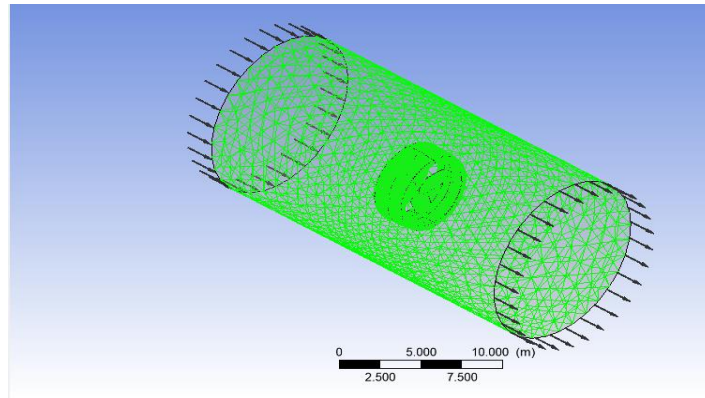


Fig. 10. Meshing

The next stage is setup (pre-processing) to create and determine parameters related to the simulation process. The steps taken during the setup process on Ansys CFX are domain and boundary [24]. This research has three domains, where the first is the fluid domain. For calm water fluid conditions, the motion domain used is stationary, while for wavy fluid conditions, the motion domain used is rotating. Next, the second is Domain Propeller, where the motion domain used is rotating in both fluid conditions. With angular velocity according to the rotation of the propeller used. And finally, the nozzle domain uses a stationary motion domain in both fluid conditions. For boundaries, a fluid domain is used, which will be the direction of fluid entry to match actual conditions. Where the inlet is visualized as the place where water enters, the wall is the place and boundary for the flow of water, and the outlet is the place where it comes out. For boundary inlets and outlets, the mass and momentum use normal speed, while for boundary walls, the mass and momentum are free slip walls, which means they move without resistance [1]. The visual results of the domain and boundary setup can be seen in Figure 11.





**Fig. 11.** Setup (Pre-Processing)

The next stage is the solver and postprocessor. At this stage, it is a calculation process (running process), with the number of iterations determined at the setup stage. The results of the solution stage (solver manager) can be seen in Figure 12. Likewise, the running results and visualization are taken as shown in Figure 13.



**Fig. 12.** Graph of solution (Solver Manager)

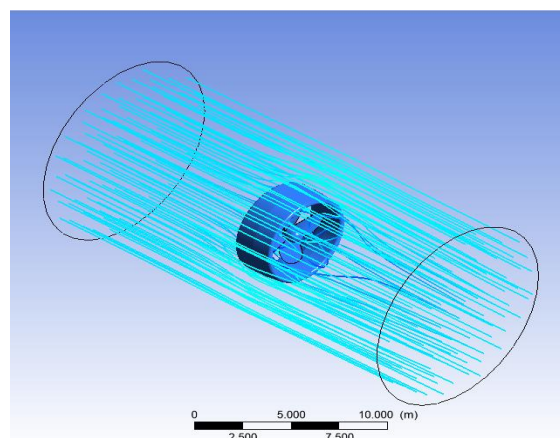


**Fig. 13.** Flow visualization

In this research, validation was carried out to find out if the stages in the simulation had been carried out correctly, so that the value and visualization of the results from the simulation were acceptable. To validate the results of the model test, use existing test results software. Validation is used to determine the appropriate domain and boundary conditions to be used in the domain and boundary conditions when analyzing three nozzle core models for the B-series propeller using CFD

software. The way to carry out validation is by comparing the thrust value from the CFD simulation results with the total resistance, where the thrust value from the simulation results must be able to meet the total propeller resistance. And also compare the manual calculation of the thrust force with the simulation results with a maximum error of 5%, which can be seen in Table 2 as follows:

**Table 2**

The thrust of validation

RPM	Simulation of result (N)	Analysis of result (N)	Error (%)	Total resistance (N)
132	308432.8	316691.01	2.607	274920.2

Based on the CFD (computer fluid dynamics) simulation process, which was carried out using Ansys CFX software, data results were obtained in the form of flow visualization, thrust force values, and propeller efficiency values in the open water test. Flow visualization is obtained from the results stage in the form of three-dimensional streamline velocity. Flow visualization in the four models can be seen in Figure 14, Figure 15, Figure 16, and Figure 17 as follows:

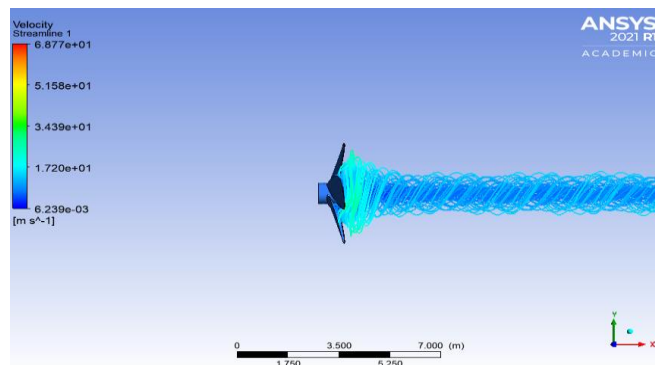


**Fig. 14.** Conventional of propeller of visualization

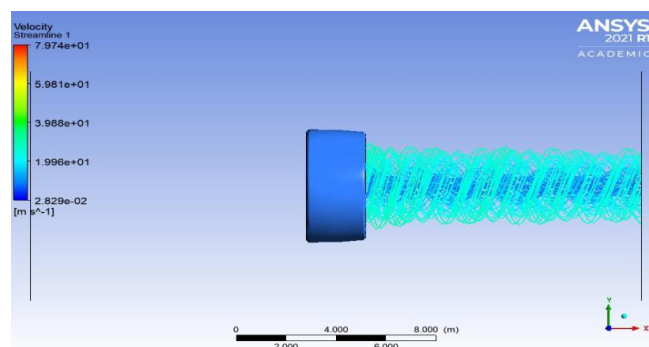


**Fig. 15.** Type A visualization



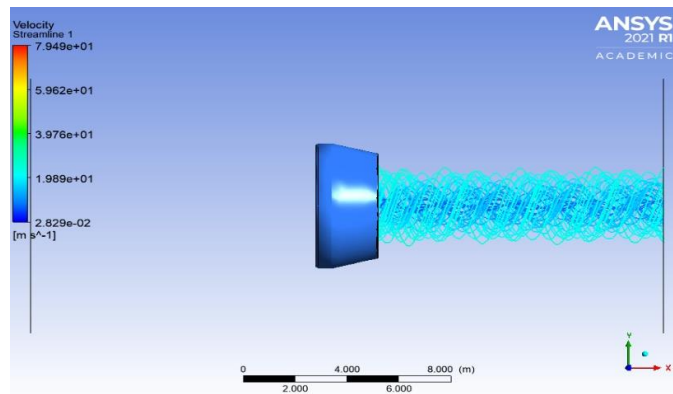


Fig. 16. Type B visualization

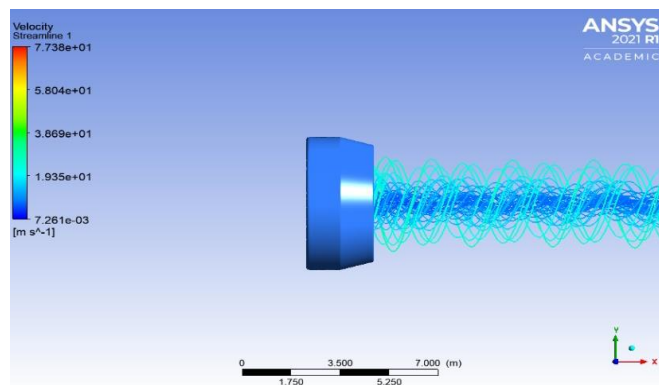


Fig. 17. Type C visualization

The CFD simulation results show that the thrust for each type of propeller without and with a cort nozzle under the influence of calm waters and wavy waters is shown in Table 3, Table 4, and Figure 18 and Figure 19 below

**Table 3**

The thrust under of calm water

RPM	Conventional (N)	Type A (N)	Type B (N)	Type C (N)
66	252901.9	317207.5	276723.2	276731.8
79	264007.6	320656.3	287579.1	287192.7
92	275113.1	324105.1	298435	297652.6
106	286219.8	327553.9	309290.9	308112.5
118	297325.3	331002.7	320146.8	318572.4
132	318432.8	334451.5	331002.7	329032.3

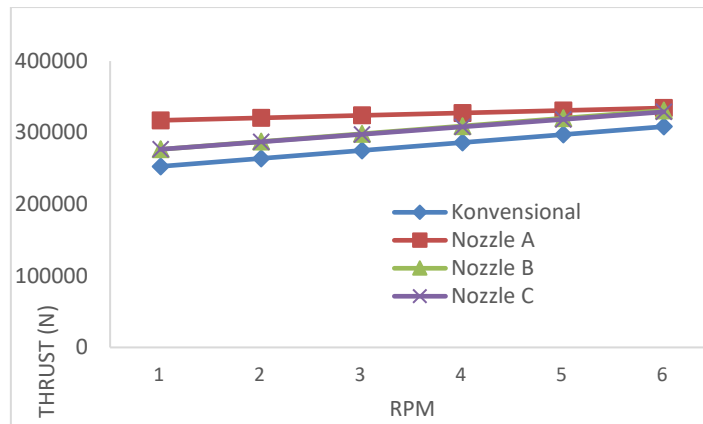


Fig. 18. The thrust of graph under of calm water

**Table 4**  
 The thrust under of wave

RPM	Conventional (N)	Type A (N)	Type B (N)	Type C (N)
66	235114.4	236306.8	246998.6	244104.3
79	247334.0	248782.5	255998.2	253824.7
92	259553.6	261258.2	265557	263545.1
106	271773.2	273733.9	275115.8	273265.5
118	283992.8	286209.6	284674.6	282985.9
132	296212.4	298685.3	294233.4	292706.3

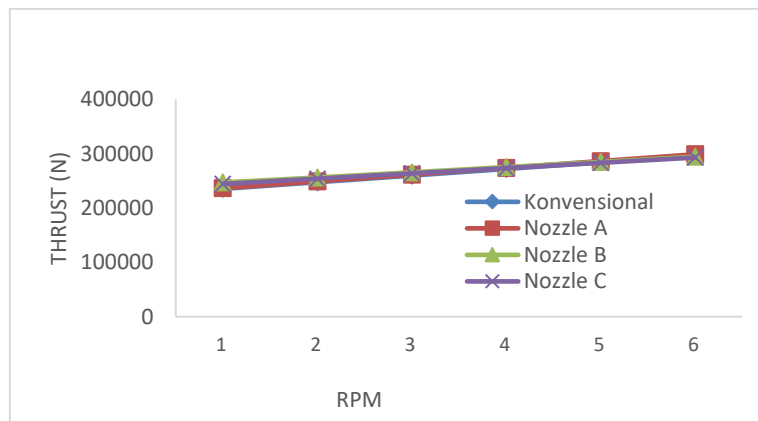


Fig. 19. The thrust of graph under of wave

Based on the results of the thrust force and torque data, the results of the open water test propeller efficiency calculations are obtained, which can be seen in Table 5, Table 6, Figure 20, and Figure 21 as follows

**Table 5**  
 The efficiency under of calm water

RPM	Type A (%)	Type B (%)	Type C (%)
66	31,3743	15,5743	22,4506
79	11,9509	7,6918	9,8108
92	6,6963	4,7893	5,8365
106	4,3368	3,3106	3,9380
118	3,1203	2,4996	2,9285
132	2,3343	1,9447	2,2544

**Table 6**  
 The efficiency under of wave

RPM	Type A (%)	Type B (%)	Type C (%)
66	0.8994	1.1083	1.0008
79	0.8688	1.0166	0.9582
92	0.6600	0.7190	0.6432
106	0.6324	0.6790	0.6754
118	0.5487	0.5782	0.5599
132	0.4804	0.4722	0.4612

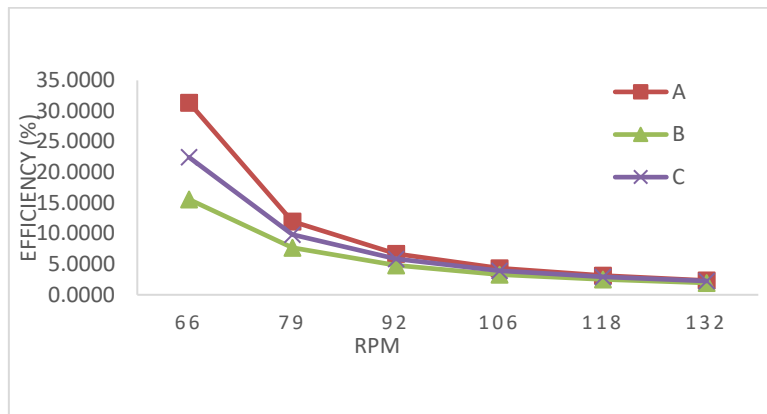


**Fig. 20.** The efficiency of graph under of calm water

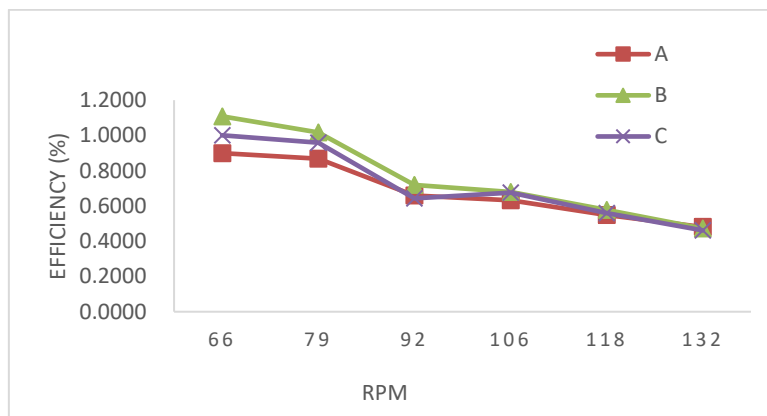


**Fig. 21.** The efficiency of graph under wave

Based on the data results in Table 5, it is known that the efficiency value of the Propeller model using type A nozzle cort is best in still water fluids. Observations started from 66 to 132 rpm. Meanwhile, Table 6 shows that the propeller with type B nozzle cort is the best in wavy fluids with the same RPM observations.

#### 4. Conclusions

It was detected that there was an increase in thrust force after using the cort nozzle under the influence of calm water and wavy water by 15 ~ 30%. there is an increase in efficiency under the influence of still water. But under the influence of waves the value is not great. The resulting efficiency value is approximately 3 ~ 5% for the same RPM rotation efficiency.

## References

- [1] Zhai, Shuo, Shuanbao Jin, Junquan Chen, Zhihua Liu, and Xiliang Song. "CFD-based multi-objective optimization of the duct for a rim-driven thruster." *Ocean Engineering* 264 (2022): 112467. <https://doi.org/10.1016/j.oceaneng.2022.112467>
- [2] Islam, Mohammed, and Fatima Jahra. "Improving accuracy and efficiency of CFD predictions of propeller open water performance." *Journal of Naval Architecture and Marine Engineering* 16, no. 1 (2019): 1-20. <https://doi.org/10.3329/jname.v16i1.34756>
- [3] Jasak, Hrvoje, Vuko Vukčević, Inno Gatin, and Igor Lalović. "CFD validation and grid sensitivity studies of full scale ship self propulsion." *International Journal of Naval Architecture and Ocean Engineering* 11, no. 1 (2019): 33-43. <https://doi.org/10.1016/j.ijnaoe.2017.12.004>
- [4] Xu, Sangming, Zhiliang Gao, and Wen Xue. "CFD database method for roll response of damaged ship during quasi-steady flooding in beam waves." *Applied Ocean Research* 126 (2022): 103282. <https://doi.org/10.1016/j.apor.2022.103282>
- [5] Kim, Daejeong, Tahsin Tezdogan, and Atilla Incecik. "A high-fidelity CFD-based model for the prediction of ship manoeuvrability in currents." *Ocean Engineering* 256 (2022): 111492. <https://doi.org/10.1016/j.oceaneng.2022.111492>
- [6] Wulandari, Amalia Ika, Mukhtar Prabu Dewanagara, Muhammad Uswah Pawara, and Syerly Klara. "Comparative Study of Rudder Performance of Single Plate and Fishtail of SPOB Ship Using CFD Method." *CFD Letters* 14, no. 5 (2022): 43-55. <https://doi.org/10.37934/cfdl.14.5.4355>
- [7] Kaewkhaw, Prachakon. "CFD investigation on steady and unsteady performances of contra-rotating propellers." *Journal of Naval Architecture and Marine Engineering* 15, no. 2 (2018): 91-105. <https://doi.org/10.3329/jname.v15i2.36225>
- [8] Henderson, R. E., J. F. McMahon, and G. F. Wislicenus. "A Method for the Design of Pumpjets." *ORL Report 63-0209* (1964). <https://doi.org/10.21236/AD0439631>
- [9] Cahyono, Bayu Sukma. "Technical analysis of nozzle correct implementation for 4990 DWT SPOB vessels on river waters." *Institut Teknologi Sepuluh Nopember*, 2016.
- [10] Schneekluth, H., and Volker Betram. *Ship design for efficiency and economy*. Butterworth-Heinemann, 1998.
- [11] Kaewkhaw, Prachakon. "CFD analysis of unsteady propeller performance operating at different inclined shaft angles for long-tail boat in Thailand." *Journal of Naval Architecture and Marine Engineering* 17, no. 2 (2020): 115-127. <https://doi.org/10.3329/jname.v17i2.42622>
- [12] Guo, Hai-Peng, and Zao-Jian Zou. "CFD and system-based investigation on the turning maneuver of a twin-screw ship considering hull-engine-propeller interaction." *Ocean Engineering* 251 (2022): 110893. <https://doi.org/10.1016/j.oceaneng.2022.110893>
- [13] Lu, Suli, Xide Cheng, Jialun Liu, Shijie Li, and Hironori Yasukawa. "Maneuvering modeling of a twin-propeller twin-rudder inland container vessel based on integrated CFD and empirical methods." *Applied Ocean Research* 126 (2022): 103261. <https://doi.org/10.1016/j.apor.2022.103261>
- [14] Franceschi, Andrea, Benedetto Piaggio, Diego Villa, and Michele Viviani. "Development and assessment of CFD methods to calculate propeller and hull impact on the rudder inflow for a twin-screw ship." *Applied Ocean Research* 125 (2022): 103227. <https://doi.org/10.1016/j.apor.2022.103227>
- [15] Aditya, Berlian Arswendo, I. Ketut Aria Pria Utama, Wasis Dwi Aryawan, and Sutiyo Sutiyo. "CFD analysis into the effect of using propeller boss cap fins (PBCF) on open and ducted propellers, case study with propeller B-series and kaplan-series." *CFD Letters* 14, no. 4 (2022): 32-42. <https://doi.org/10.37934/cfdl.14.4.3242>
- [16] Timushev, Sergey, Alexey Yakovlev, and Dmitry Klimenko. "CFD-CAA Method for Prediction of Pseudosound and Emitted Noise in Quadcopter Propeller." *International Journal of Modeling and Optimization* 12, no. 1 (2022): 21-25. <https://doi.org/10.7763/IJMO.2022.V12.794>
- [17] Setiawan, Wira, Amalia Ika Wulandari, Aditya Miftahul Huda, and Syerly Klara. "Comparative Study of Ship Resistance and Fuel Consumption between Axe Bow and Moor Deep Ram Bow using CFD Method." *CFD Letters* 14, no. 8 (2022): 71-80. <https://doi.org/10.37934/cfdl.14.8.7180>
- [18] Wulandari, Amalia Ika, I. Ketut Aria Pria Utama, Afifah Rofidayanti, and Dominic Hudson. "Numerical Analysis of Ship Motion of Crew Boat with Variations of Wave Period on Ship Operational Speed." *CFD Letters* 16, no. 4 (2024): 1-15. <https://doi.org/10.37934/cfdl.16.4.115>
- [19] Ansys. "Academic research mechanical." *ANSYS Inc.*, 2021.
- [20] Jangam, Suneela. "CFD based prediction on hydrodynamic effects of Interceptor and flap combination on planing hull." *Ocean Engineering* 264 (2022): 112523. <https://doi.org/10.1016/j.oceaneng.2022.112523>
- [21] Ma, Chengqian, Takanori Hino, Ning Ma, and Youhei Takagi. "CFD investigation on the hydrodynamic loads and motions when ship maneuvers in regular and irregular waves." *Ocean Engineering* 266 (2022): 113040.

- <https://doi.org/10.1016/j.oceaneng.2022.113040>
- [22] Dentale, Fabio, Ferdinando Reale, Angela Di Leo, and Eugenio Pugliese Carratelli. "A CFD approach to rubble mound breakwater design." *International Journal of Naval Architecture and Ocean Engineering* 10, no. 5 (2018): 644-650. <https://doi.org/10.1016/j.ijnaoe.2017.10.011>
- [23] Fitriadhy, Ahmad, Nur Amira Adam, Izzati Pison, Mohd Asamudin A. Rahman, Mohd Azlan Musa, and Mohd Hairil Mohd. "Computational Investigation into Resistance Characteristic of A Pusher-Barge System." *Journal of Naval Architecture & Marine Engineering* 18, no. 2 (2021): 241-254. <https://doi.org/10.3329/jname.v18i2.52593>
- [24] Ravenna, Roberto, Soonseok Song, Weichao Shi, Tonio Sant, Claire De Marco Muscat-Fenech, Tahsin Tezdogan, and Yigit Kemal Demirel. "CFD analysis of the effect of heterogeneous hull roughness on ship resistance." *Ocean Engineering* 258 (2022): 111733. <https://doi.org/10.1016/j.oceaneng.2022.111733>